PHILOSOPHICAL TRANSACTIONS OF THE ROYAL SOCIETY A MATHEMATICAL, PHYSICAL & ENGINEERING SCIENCES

Palaeomagnetism, North China and South China Collision, and the Tan-Lu Fault

Jin-Lu Lin and M. Fuller

Phil. Trans. R. Soc. Lond. A 1990 **331**, 589-598
doi: 10.1098/rsta.1990.0091

Phil. Trans. R. Soc. Lond. A **331**, 589–598 (1990)
Printed in Great Britain

Palaeomagnetism, North China and South China collision, and the Tan-Lu fault

By Jin-Lu Lin and M. Fuller

Department of Geological Sciences, University of California, Santa Barbara, California 93106, *U.S.A.*

Refined Apparent Polar Wander (APW) paths for the North and South China Blocks (NCB and SCB) are presented and the collision between the NCB and SCB discussed. We suggest that the amalgamation of the NCB and SCB was completed in the late Triassic–early Jurassic, during the Indosinian Orogeny. This proposed timing is based on an analysis of palaeomagnetic signatures relating to continental collisions, such as the convergence of palaeolatitude, deflections of declination, hairpin-like loops in and superposition of APW paths. Like the Cenozoic India–Eurasia collision, the Mesozoic NCB–SCB collision reactivated ancient faults in eastern China, converting some of them into transcurrent faults, of which the Tan-Lu fault is the most famous.

Introduction

The NCB and SCB are two of the major blocks in eastern Asia (figure 1). It is now generally agreed that these two blocks were separated from each other in the geological past, and that they collided later to give rise to the Qinling foldbelt. However, the question of when they finally amalgamated has been a matter of debate (Mattuaer *et al.* 1985; Sengor 1985; Hsu *et al.* 1987; Lin *et al.* 1985; Zhao & Coe, 1987). The Tan-Lu fault is a major transcurrent fault in eastern Asia on which a large displacement took place in the early Mesozoic (Xu *et al.* 1987), but the mechanism for its reactivation and displacement has not been clarified.

In this paper we discuss the palaeomagnetic data from the NCB and SCB, examine the palaeomagnetic signatures relating to continental collision, and provide palaeomagnetic constraints on the timing and style of the NCB–SCB collision. Finally, we discuss the relationship between the NCB–SCB collision and the Tan-Lu fault.

Palaeomagnetic data

All presently available palaeomagnetic results for the NCB and SCB are summarized in table 1, and their APW paths are depicted in figure 2. Detailed documentation of the database used here has been published in Chinese journals (Lin 1987, 1989). The new data for the NCB and the new Mesozoic data for the SCB reported by several groups are generally in agreement with each other, and also in agreement with the preliminary APW paths (Lin *et al.* 1985). Here we discuss only the controversial Permian and Tertiary results, and comment on a recently published late Triassic result from the SCB (Zhu *et al.* 1988).

A recent study of some Palaeocene–Eocene sediments yields a pole close to the present north pole (Zhuang *et al.* 1988). This is in conflict with the previous Neogene pole. Moreover, this previous Neogene pole gives rise to a kink in the Neogene APW path. This kink contradicts the generally accepted notion that APW paths are composed of a series of small circles, such as we

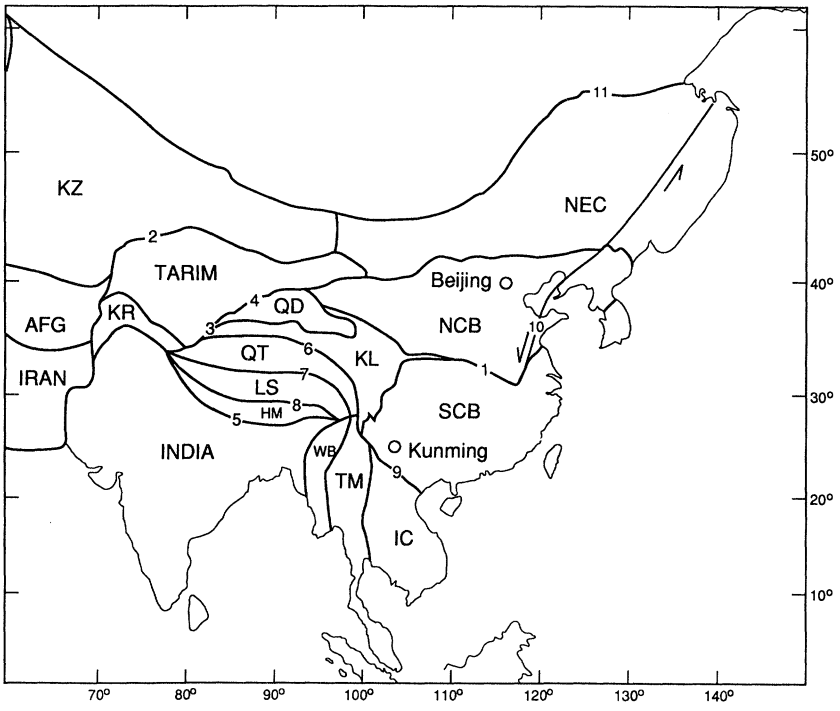

FIGURE 1. Blocks and terranes in China and East Asia (Mercator projection). Abbreviations are as follows. AFG, Afghanistan Terrane; HM, Himalayan Terrane; IC, Indochina Block; IRAN, Central Iran Terrane; KL, Kunlun Terrane; KR, Karakoram Terrane; KZ, Kazakhstan Block; LS, Lhasa Terrane; NCB, North China Block; NEC, Northeast China composite terrane; QD, Qaidam Terrane; QT, Qiangtang Terrane; SCB, South China Block; TM, Thai-Malay Terrane; WB, West Burma Terrane. 1. Qinling-Dabie suture; 2. Tien Shan Mountains; 3. Kunlun Mountains; 4. Altyn Tagh fault; 5. Main boundary thrust (MBT); 6. Jinsha suture; 7. Banggong–Nujiang suture; 8. Indus-Zangpo suture; 9. Red River fault. 10. Tan-Lu fault; 11. Mongol–Okhotsk foldbelt.

see on the APW paths for North America and northern Eurasia, which are the two best defined APW paths at present (Gordon *et al.* 1984). As the earlier Neogene pole is based only on three lava flows and an early result from redbeds which were subjected solely to alternating field (AF) demagnetization, we prefer to exclude our Neogene pole from the APW path until additional data justify its inclusion.

Zhu *et al.* (1988) have reported late Triassic results (table 2), which exhibit pronounced streaking along a small circle about the sampling localities, and clearly do not have a fisherian distribution (figure 3). These results differ from each other mainly in declination, but not in inclination. This probably reflects differential rotations at various sampling localities. A statistical analysis of inclination alone based on the method of McFadden & Reid (1982) yields a mean palaeolatitude of $20.1° \pm 2.3°$. When a small circle with a radius of 69.9° is drawn about the average sampling centre (27° N, 102° E), it intersects with the APW path for the SCB, and the intersection point falls between the middle Triassic and middle Jurassic poles (figure 3). We suggest that it is not the overall mean (mean A in table 2), but the mean B which is calculated on the palaeopoles close to the intersection point, most likely represents the late Triassic palaeopole position of the SCB.

The Permian result from the Emeishan basalts by McElhinny *et al.* (1981) was initially not included in the preliminary APW path for the SCB because of the possibility of remagnetization.

Table 1. Palaeomagnetic data from the North and South China Blocks

no.	age	Ma	palaeopole lat. N	palaeopole lon. E	K	A95	B	Test	palaeolatitude Ob	palaeolatitude Ex
			A. The South China Block						Kunming	Beijing
1	N	10	74.2	36.5	148	7.6	8	R	30.3	41.0
2	E1–E2	53	85.2	174.6	46	(11.9)	6	R	26.4	42.4
3	K2–E1	65	76.3	172.6	23	10.3	10	F	29.0	46.4
4	K1–Km	100	67.6	205.1	35	5.8	19	FR	18.6	36.8
5	K1	125	76.2	225.7	662	4.8	[3]	R	17.1	34.2
6	J3	140	73.0	213.7	29	12.6	6		18.1	35.8
7	J2	165	71.5	201.1	135	5.8	6	R	21.1	39.1
8	Tr3	215	63.9	198.4	530	3.3	5	F	20.0	38.4
9	Tr2	235	54.6	209.7	95	(5.7)	2	RF	11.2	29.7
10	P2–Tr1	250	48.4	219.7	215	4.6	[6]	FR	2.6	21.1
11	P	260	28.5	226.6	112	11.7	3	R	−13.8	4.0
12	C	320	22.2	223.8	83	8.5	5	R	−15.7	1.5
13	D2	380	−8.9	190.4	13	6.9	7	F	−1.4	6.0
14	S2	425	6.8	195.6	122	4.0	12	F	0.5	12.3
15	Є1	560	3.4	195.0	28	8.8	8	RF	−0.4	10.6
			B. The North China Block						Beijing	
1	N	20	80.6	183.1	91	7.1	6	R	43.1	
2	K2	80	69.0	182.0	193	4.0	8		45.4	
3	K1	115	69.0	200.0	40	12.2	5	R	39.0	
4	J3	140	72.8	214.6	426	6.0	[3]		35.5	
5	J2	165	81.0	238.0	194	8.9	[3]		34.8	
6	Tr2	235	48.9	22.1	418	12.3	[2]	R	26.8	
7	P2–Tr1	250	38.6	9.0	339	5.0	[4]	RF	13.0	
8	P2	255	48.8	0.9	176	9.3	[3]	R	15.6	
9	O2	455	43.2	332.5	53	(10.6)	1		−0.5	
10	O	475	29.1	305.8	18	18.6	5	R	−20.3	
11	Є1	560	15.0	298.6	38	9.9	7	R	−34.9	
12	Z2	570	16.5	301.1	35	9.5	8	R	−33.3	

(Geological time abbreviations: N, Neogene; E, Eogene (Palaeogene); K, Cretaceous; J, Jurassic; Tr, Triassic; P, Permian; C, Carboniferous; D, Devonian; S, Silurian; O, Ordovician; Є, Cambrian; Z, Sinian (*ca.* 850–570 Ma). Early, middle and late epochs of geological periods are denoted with subscripts 1, 2, and 3 respectively. Numerical ages in million years (Ma) are estimated ages obtained by referring the relative stratigraphic levels of sampling formations to the Geological Time Scale (Snelling 1987). K is the precision parameter of the Fisher statistics. A95 is the radius of 95% error circle about the mean palaeopole, or the semi-angle of 95% error about the mean direction when it is in parentheses. B is the number of sites, or number of localities when in brackets. In the test column, R represents the reversal test, F the fold test, and C the contact test. In addition to the observed palaeolatitudes (Ob) of Kunming and Beijing, the expected palaeolatitude (Ex) of Beijing is also calculated relative to the palaeopoles of the SCB. The present geographic coordinates of the two chosen reference points are: Beijing (40° N, 116° E), and Kunming (25° N, 103° E). Sources of data: A. the South China Block: no. 1. Lin *et al.* (1985); 2. Zhuang *et al.* (1988); 3. Kent *et al.* (1986); 4. Lee *et al.* (1987); 5–7. Lin *et al.* (1985); 8. Zhu *et al.* (1988); 9. Chan *et al.* (1984); 10. Lin *et al.* (1985), Opdyke *et al.* (1986), Zhang (1984), Li *et al.* (1989), Steiner *et al.* (1989); 11. Lin (1987*b*), Lin *et al.* (1985), Zhou *et al.* (1986); 12. Lin *et al.* (1985); 13. Fang *et al.* (1989); 14. Opdyke *et al.* (1987); 15. Lin *et al.* (1985); B. the North China Block: no. 1. Lin *et al.* (1985), Zhao (1987); 2, 3. Lin *et al.* (1985); 4. Lin (1987*a*); 5. Lin (1987*a*), Cheng *et al.* (1988), Fang *et al.* (1988); 6. Cheng *et al.* (1988), Fang *et al.* (1988); 7. Lin (1987*a*), Cheng *et al.* (1988), McElhinny *et al.* (1981); 8. McElhinny *et al.* (1981), Zhao and Coe (1987); 9. Lin *et al.* (1985); 10. Zhao (1987); 11, 12. Lin *et al.* (1985).)

Several new studies have been carried out since then. A recent reinterpretation of these data proposes a predominant normal or mixed polarity of these mid and late Permian basalts (Zhou *et al.* 1986; Zhao & Coe 1987). However, the normal polarity directions from the Emeishan basalts are questionable for the following reasons. (1) The natural remanent magnetization

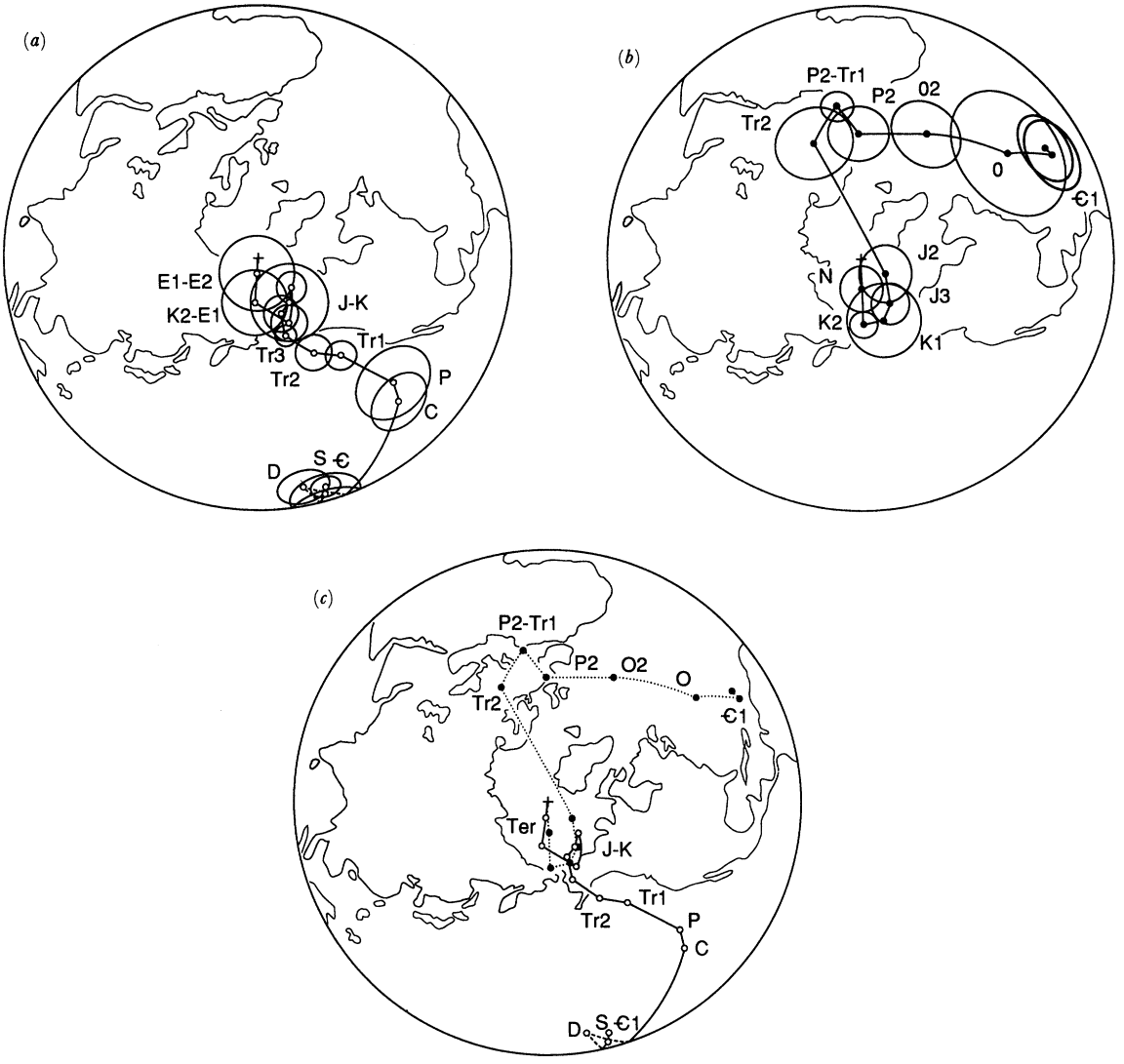

FIGURE 2. The APW paths for (*a*) South China Block, and (*b*) for North China Block, and (*c*) their superposition. Open circles represent palaeopoles from SCB, whereas solid circles those from NCB. Jurassic and Cretaceous poles from SCB are collectively denoted by J-K. Tertiary poles are indicated by Ter. See table 1 for all other abbreviations of geological ages.

(NRM) of the basalts from the Emeishan section consists of a single component of which the *in situ* direction ($D/I = 2.3°/29.2°$) is close to the local dipole field direction (McElhinny *et al.* 1981). (2) The normal and reversed directions are not antipodal but 157.5° away from each other, so that they fail a reversal test (Lin 1989). (3) Although there is a positive fold test, as the folding took place in the latest Cretaceous–Tertiary, so that a Mesozoic remagnetization cannot be precluded. (4) Palaeontological stratigraphy places the Emeishan basalts in the mid-Permian and not latest Permian. The frequently cited isotopic age of 237 Ma of the basalts, if accepted, brings the stratigraphic level of the Emeishan basalts up to the middle Triassic, in evident contradiction with the Permian index fossils in the limestones which are sandwiched by the Emeishan basalts. (5) Steiner *et al.* (1989) have recently obtained some new results from four biostratigraphically well studied uppermost Permian–lowest Triassic sections in eastern

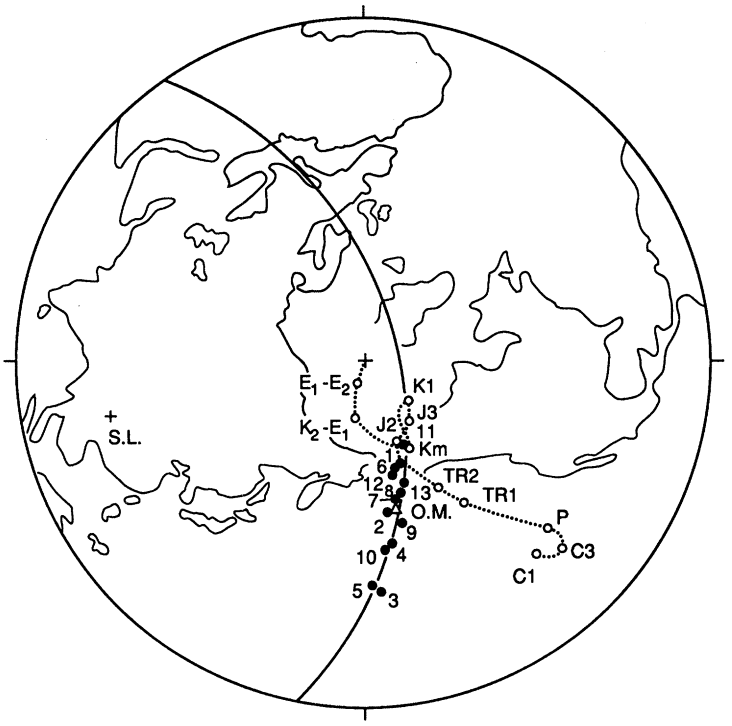

FIGURE 3. Late Triassic palaeopoles from western South China. S.L., sampling locality. Small dot represents palaeopole from each site. O.M., the overall mean (triangle) of the 13 site-palaeopoles. Part of the APW path for the SCB is also shown. Notice that the 13 palaeopoles fall on a small circle centred at the sampling locality and with a radius of 69.9°. Also notice that this small circle intersects the APW path between the middle Triassic and middle Jurassic poles. We suggest that it is this intersection point, rather than the fisherian overall mean, which more likely gives the late Triassic pole position.

TABLE 2. UPPER TRIASSIC RESULTS FROM WESTERN SICHUAN AND CENTRAL YUNNAN

	locality			direction				palaeopole			
no.	lat. N	lon. E	*N*	dec.	inc.	*K*	a95	lat. N	lon. E	dp	dm
1*	28.3	103.0	7	28.6	41.3	13	14.6	63.9	198.0	10.8	17.7
2	—	—	6	40.6	43.6	10	18.0	53.9	188.5	14.0	22.5
3	26.6	101.7	6	61.4	36.1	80	6.4	33.7	184.3	4.3	7.4
4	—	—	6	48.2	37.2	11	17.6	45.7	187.8	12.0	20.7
5	—	—	5	59.9	40.2	35	10.6	36.0	181.7	7.7	12.8
6*	26.8	101.5	6	27.4	37.5	11	17.6	64.4	197.6	12.2	20.8
7	—	—	5	35.8	38.2	9	20.9	57.0	193.7	15.2	25.6
8	—	—	5	34.7	37.3	66	7.7	57.8	195.1	5.3	9.0
9	26.4	102.4	6	41.5	35.6	35	9.6	51.4	192.8	6.4	11.1
10	—	—	6	49.5	39.4	30	10.4	45.0	186.3	7.4	12.4
11*	25.1	101.9	6	34.5	22.3	119	5.2	68.4	204.7	3.4	6.0
12*	—	—	5	37.6	29.3	41	9.8	62.8	194.7	6.8	11.5
13*	—	—	5	34.2	32.1	64	8.7	59.6	198.1	5.7	9.9
A.	overall mean		13	—	—	49	6.0	54.0	191.1	—	—
B.	mean (*)		5	—	—	530	3.3	63.9	198.4	—	—
C.	mean		13	—	36.2	106	3.4	palaeolatitude = 20.1° ± 2.3°			

(Lat. N, northern latitude; lon. E, eastern longitude; dec., declination; inc., inclination; *N*, the number of samples; *K*, the precision parameter of the Fisher statistics; a95, the half-angle of 95% confidence cone about mean direction; dp and dm, the semi-axes of 95% polar error. No. 1–10 are from western Sichuan, and 11–13 from central Yunnan. No. 1, 2 are from the Xujiahe Formation, 3–5 from the Bingnan Formation, and 6–10 from the Baigewan formation. Results from these three formations pass the general fold test (or tectonic test) at 95%. No. 11–13 are from the Yipinglang area. All samples are from sedimentary rocks. Three means are given in the table, where A is the overall mean, B is a selective mean based on five sites (1, 6, 11–13), and C is a mean based on inclinations only (McFadden & Reid 1982). The original data are from Zhu *et al.* (1988).)

Sichuan, some 200 km away from the Emeishan basalt section. By combining their results with those of Opdyke *et al.* (1986), they give a mean palaeopole at 46.1° N, 223.6° E for the latest Permian–earliest Triassic, which is about 20° away from the palaeopole (49° N, 251° E) for the time interval suggested by Zhao & Coe (1987). Moreover, including the late Permian pole calculated from the normal polarity directions destroys the originally curvilinear feature of the APW path from the Permo–Carboniferous to the late Triassic, and gives rise to a kink in the path. Using the Permian pole in table 1 which is calculated from the reversed polarity direction alone (Lin *et al.* 1985; Zhou *et al.* 1986; Lin 1987*b*), no kink appears on the APW path. A more detailed discussion of this point has recently been given by Lin (1989).

Palaeomagnetic signatures of continental collisions

Palaeomagnetic signatures of continental collisions include: (1) palaeolatitudinal convergence of colliding blocks, (2) deflection of remanent declinations, (3) hairpin-like loops on the APW paths for colliding blocks, and (4) convergence of APW paths upon collision followed by superposition of the paths after complete amalgamation of colliding blocks. These palaeomagnetic signatures, especially when used collectively, provide important constraints on the timing and tectonic style of continental collisions.

Palaeomagnetism can be most readily applied to the study of the timing and style of continental collisions when the following conditions are satisfied. (1) The collision has taken place within the time for which high-resolution palaeomagnetic results can be obtained. For example, the last collision between North America and Europe took place in the Devonian and led to the Caledonian Orogeny. As the early Palaeozoic palaeomagnetic data from the two continents are still somewhat controversial, it makes a detailed study of palaeomagnetic signature of the Caledonian Orogeny difficult. (2) The two colliding blocks should be large enough in size to provide relatively complete stratigraphic sequences so that sufficiently detailed APW paths can be constructed. The terranes defined in Northwest America do not usually provide complete APW paths, say, since the early Mesozoic (Howell 1985), so that it is hard to unravel collisional history. (3) The post-collisional deformation within the continents and along the collisional boundary should not be so severe that the pre- and syn-collisional palaeomagnetic signatures are totally destroyed by the later deformation. For example, the India–Eurasia collision is difficult to analyse, because there is a large amount of post-collisional crustal shortening in the Tibetan Plateau and along the main central thrust (MCT) and main boundary thrust (MBT). In this case, the shortening along the MBT alone is estimated as 300–500 km or even 800 km (Dewey *et al.* 1988). (4) The necessary palaeomagnetic data must be available from the colliding blocks. (5) The geology and tectonics of colliding blocks should be well documented so that a cross check of geology and palaeomagnetism is possible.

Judging by these five criteria, the collision between the NCB and SCB is suitable for analysis by palaeomagnetic signatures. The SCB contains a complete Phanerozoic sequence, as does the NCB with the exception of the hiatus from the upper Ordovician to the lower Carboniferous. It has been suggested that the collision between them occurred during the Indosinian Orogeny, in the late Triassic and early Jurassic. Palaeomagnetic data for the Permian, Triassic, Jurassic, Cretaceous and Tertiary from the two blocks are available and generally considered reliable, so that the post-Carboniferous APW paths are available for both blocks. The post-collisional deformation within the two blocks and along their suture zone, the Qinling foldbelt, is far less

severe than in Tibet and the Himalayas. Finally, the NCB and SCB and the Qinling foldbelt are *terra cognita* geologically. This encourages us to choose the NCB and SCB as a test site to examine the value of the proposed palaeomagnetic signatures in analysis of collision and to gain constraints on the timing and tectonic style of the NCB–SCB collision.

PALAEOLATITUDINAL CHANGE

Figure 4 shows the palaeolatitudinal change of the NCB and SCB, with the cities of Beijing and Kunming chosen as reference sites for the NCB and SCB, respectively. We define the *observed palaeolatitude* for a site, e.g. Beijing, as the latitude which is calculated based on a palaeopole from the block (NCB) on which the site is located, and define the *expected palaeolatitude* as the one calculated from the palaeopole of the other block (SCB). If there had been no relative motion between the NCB and SCB, the expected and observed palaeolatitudes of Beijing should be consistent with each other. On the other hand, if the two palaeolatitude values are different, this indicates that significant relative poleward motion has taken place between the two blocks.

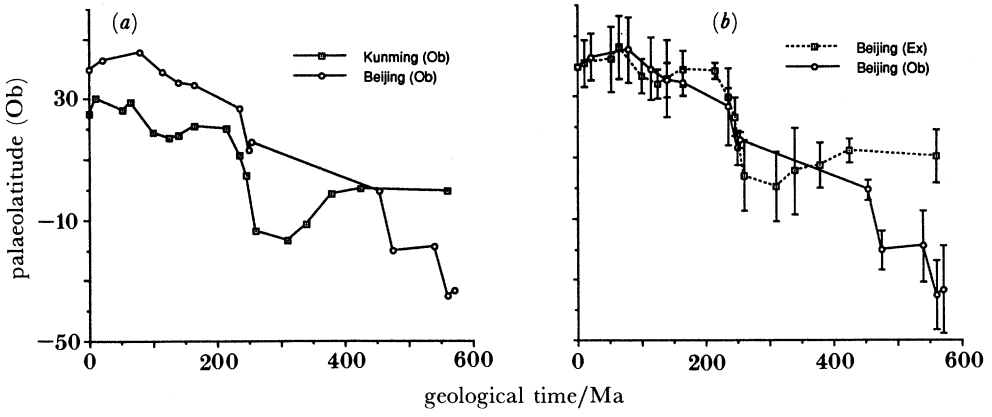

FIGURE 4. (*a*) Observed palaeolatitudinal changes of Beijing in the NCB and of Kunming in the SCB. (*b*) Comparison of the observed and expected palaeolatitudinal values of Beijing. Dashed line represents the expected palaeolatitude of Beijing relative to the palaeopoles of the SCB. Vertical bars are 95% confidence intervals (A95). The two curves are quite different in the early Palaeozoic, but become virtually indistinguishable after the beginning of the Triassic. Plots are based on the data listed in table 1. Palaeomagnetic data are not available for the NCB in the Silurian, Devonian and Carboniferous.

We see in figure 4 that the observed and expected palaeolatitudinal curves of Beijing are superposed since Triassic, but differ significantly in the early Palaeozoic and also in the Permian. This indicates that there has been considerable relative motion between the two blocks since Cambro–Ordovician time. The palaeolatitudes approached each other in the late Permian, became similar in the Triassic. No significant relative poleward motion has taken place since then. These observations suggest that the collision between the NCB and SCB occurred in the Triassic, or the so-called Indosinian Orogeny. Unfortunately, the above interpretation is weakened by the lack of palaeomagnetic results of the Carboniferous, Devonian and Silurian times from the NCB. We therefore turn to other palaeomagnetic signatures.

Rapid deflection of remanent declination

Continental collisions are likely to start at promontories because they form irregularities in the continental outlines (see, for example, Wilson 1966). The two plates may then rotate towards each other as the collision proceeds, or the promontories may rotate to become parallel to the main collision front. Thus collisions are likely to lead to rapid rotations, which give rise to rapid changes in declination without accompanying changes in inclination. In an APW path this gives rise to an arc of a small circle about the site. As we mentioned above, from the Triassic the observed and expected palaeolatitudes of Beijing become consistent with each other, so that the relative change in inclinations of the two blocks essentially stopped. However, a big change in the declination of the NCB started shortly after in the late Triassic. The declination of the early and middle Triassic is about N45° W, but becomes N15° E in the middle Jurassic, indicating 60° counterclockwise (CCW) rotation of the remanent magnetization vector. We interpret this rotation to be related to the collision between the NCB and SCB. We speculate that before the collision the NCB, together with Mongolia–Northeast China, formed a promontory to the south of the Siberian Platform, perhaps similar to the present Malayian peninsula relative to the Asian continent. With the collision of the SCB, the tectonic assemblage of the NCB–Mongolia–Northeast China rotated CCW by 60° into approximately its present configuration with respect to Siberia. This finally closed the Mongol–Okhotsk remnant ocean between Mongolia–Northeast China and the Siberian Platform. There is no comparable rotation recorded for the SCB during the Triassic–Jurassic time. The NCB and SCB must therefore have been still moving somewhat independently at that time and did not form a coherent tectonic entity in middle Triassic time, although their initial collision had probably started by then.

Smooth tracks and hairpin-like loops in APW paths

APW paths often consist of curvilinear arcs, or tracks, and hairpin-like loops. Tracks indicate uniform, relatively rapid plate motion whereas loops indicate stagnation of polar wander, suggesting confrontation with obstacles in plate motion, most likely, continental collisions (Irving & Park 1972; Gordon *et al.* 1984). The APW path for the SCB has a substantial linear segment from the late Carboniferous to the late Triassic, representing rapid and uniform APW during that time. However, this APW was halted during the late Triassic and is much less rapid in the Jurassic and Cretaceous. There may be a loop in the APW path, although the detailed form of the curve is beyond the resolution of the available data. We interpret this Jurassic–Cretaceous loop, or stagnation point, on the APW path for the SCB as evidence for a continental collision. We suggest that the collision was with the NCB.

Superposition of APW paths

The two APW paths for the NCB and SCB are plotted on the same map in figure 2*c*. They are widely separated in the Palaeozoic, start to approach each other in the early Mesozoic, meet in the middle Jurassic and are indistinguishable subsequently. This indicates that the amalgamation of the two blocks was not accomplished until as late as the early Jurassic, which again indicates an Indosinian collision.

NCB–SCB COLLISION AND DISPLACEMENT ON THE TAN-LU FAULT

Continental collisions may reactivate ancient faults in continents, sometimes converting them into transcurrent faults on which a large amount of strike–slip motion takes place. The Cenozoic tectonics in Asia following the India–Eurasia collision affords the best known example of this behaviour (Molnar & Tapponnier 1975). In the eastern continental margin of Asia the Tan-Lu is the largest and most important fault on which a major displacement started in the late Triassic, i.e. during the Indosinian Orogeny (Xu *et al.* 1987). We suggest that the reactivation of, and displacement on, the Tan-Lu fault is directly related to the collision between NCB and SCB. The present trends of the Tan-Lu fault and the Qinling suture zone between NCB and SCB are nearly orthogonal (figure 1). However, on a middle Triassic map reconstructed based on palaeomagnetic data, the strike of the Tan-Lu fault becomes nearly parallel to the relative motion vector of SCB upon its collision with NCB (figure 5). This palaeogeometry suggests that due to the continental collision and continued northward drive of SCB after the collision, ancient faults in eastern NCB, such as the Tan-Lu fault, were reactivated or converted into left-lateral strike–slip faults.

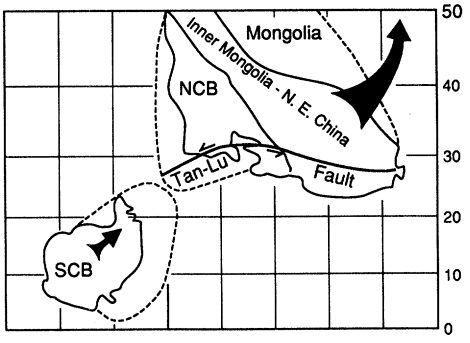

FIGURE 5. A middle Triassic reconstruction map of SCB and NCB, showing their palaeo-orientations as well as their palaeolatitudes. Notice that the northern margin of SCB was parallel to the incipient Tan-Lu fault. This suggests that there may be a relation between the SCB–NCB collision in the one hand, and the reactivation of and displacement on the Tan-Lu fault in the other hand. We suggest that the push from SCB may be strong enough to force the assemblage of NCB–Mongolia–Northeast China to have rotated counterclockwise and thus to have brought the Mongol–Okhotsk palaeo-ocean into final closure.

CONCLUSION

In conclusion, we note that a variety of collision-related palaeomagnetic signatures suggest an Indosinian collision between NCB and SCB. The palaeolatitudes of NCB and SCB converge in the Triassic. There is a rapid change in declination of up to 60° of NCB during the late Triassic and early Jurassic. In the two APW paths there is a Jurassic–Cretaceous hairpin-like loop or stagnation point. Finally, post-Middle Jurassic APW paths for the two blocks are indistinguishable. All of these palaeomagnetic signatures suggest that the collision between the NCB and SCB started in the early or middle Triassic time, and was completed in the late Triassic–early Jurassic time. This is consistent with various lines of geological evidence (Hsu *et al.* 1987), such as the characteristic stratigraphic sequences in the Qinling foldbelt, the Sm–Nd age determination of the collision-related C-type eclogite (Li *et al.* 1989), the radiometric age dating of granitic batholiths in the Qinling foldbelt and so on. The collision model

which we propose predicts that the collision of the NCB–Mongolia-Northeast China assemblage with Siberia should begin in the west and progress eastward, while that of the SCB with NCB should start towards the east and progress westward.

References

Chan, L. S., Wang, C. Y. & Wu, X. Y. 1984 *Geophys. Res. Lett.* **11**, 1157–1160.
Cheng, G., Bai, Y. & Sun, Y. 1988 *Seismol. Geol.* **10**(2), 81–87.
Dewey, J. F., Shackleton, R. M., Chang, Ch. & Sun, Y. 1988 *Phil. Trans. R. S. Lond.* A**327**, 379–413.
Fang, D., Guo, Y., Wang, Zh., Tan, X., Fan, Sh., Yuan, Y., Tang, X. & Wang, B. 1988 *Kexue Tongbao* **33**(2), 133–135.
Fang, W., Van der Voo, R. & Liang, Q. 1989 *Tectonics* **8**, 939–952.
Gordon, R. G., Cox, A. & O'Haire, S. 1984 *Tectonics* **3**, 499–537.
Howell, D. G. (ed.) 1985 *Tectonostratigraphic terranes of the Circum-Pacific region*. Circum-Pacific Council for Energy and Mineral Resources, Houston, Texas, U.S.A. (581 pages.)
Hsu, K. J., Wang, Q., Li, J., Zhou, D. & Sun, Sh. 1987 *Eclogae Geol. Helv.* **80**, 735–752.
Irving, E. & Park, J. K. 1972 *Can. J. Earth Sci.* **9**, 1318–1324.
Kent, D. V., Xu, G., Huang, K., Zhang, W. Y. & Opdyke, N. D. 1986 *Earth planet. Sci. Lett.* **79**, 179–184.
Lee, G., Besse, J., Courtillot, V. & Montigny, R. 1987 *J. geophys. Res.* B**92**, 3580–3596.
Li, H., Wang, J., Heller, F. & Lowrie, W. 1989 *Chin. Sci. Bull.* **34**, 431–434.
Li, Sh., Ge, N., Liu, D., Zhang, Z., Ye, X., Zheng, Sh. & Peng, Ch. 1989 *Kexue Tongbao* **33**, 522–525.
Lin, J. 1987*a* *Scientia Geol. Sin.* **2**, 183–187.
Lin, J. 1987*b* *Scientia Geol. Sin.* **4**, 306–315.
Lin, J. 1988 *Seismol. Geol.* **10**(3), 1–11.
Lin, J. 1989 *Geol. Rev.* **35**, 349–354.
Lin, J., Fuller, M. & Zhang, W. 1985 *Nature, Lond.* **313**, 444–449.
Mattauer, M., Matte, Ph., Malavieille, J., Tapponnier, P., Maluski, H., Xu, Zh., Lu, Y. & Tang, Y. 1985 *Nature, Lond.* **317**, 496–500.
McElhinny, M. W. 1985 *J. Geodynamics* **2**, 115–117.
McElhinny, M. W., Embleton, B. J. J., Ma, X. H. & Zhang, Z. K. 1981 *Nature, Lond.* **293**, 212–216.
McFadden, P. L. & Reid, A. B. 1982 *Geophys. Jl R. astr. Soc.* **69**, 307–319.
Molnar, P. & Tapponnier, P. 1975 *Science, Wash.* **189**, 419–426.
Opdyke, N. D., Huang, K., Xu, G., Zhang, W. & Kent, D. V. 1986 *J. geophys. Res.* B**91**, 9553–9568.
Opdyke, N. D., Huang, K., Xu, G., Zhang, W. Y. & Kent, D. V. 1987 *Tectonophysics* **139**, 123–132.
Sengor, A. M. C. 1985 *Nature, Lond.* **318**, 16–17.
Snelling, N. J. 1987 *Modern Geol.* **11**, 365–374.
Steiner, M., Ogg, J., Zhang, Z. & Sun, S. 1989 *J. geophys. Res.* **94**, 7343–7363.
Wilson, J. T. 1966 *Nature, Lond.* **211**, 676–681.
Xu, J., Zhu, G., Tong, W., Cui, K. & Liu, Q. 1987 *Tectonophysics* **134**, 273–310.
Zhang, Zh. 1984 *Bull. Chi. Acad. Geol. Sci.* **9**, 45–54.
Zhao, X. 1987 Ph.D. thesis, University of California at Santa Cruz, U.S.A.
Zhao, X. & Coe, R. C. 1987 *Nature, Lond.* **327**, 141–144.
Zhou, Y., Lu, L. & Zhang, B. 1986 *Geol. Rev.* **32**, 465–469.
Zhu, Zh., Hao, T. & Zhao, H. 1988 *Acta Geophys. Sin.* **31**, 420–431.
Zhuang, Zh., Tian, D., Ma, X., Ren, X., Jiang, X. & Xu, Sh. 1988 *Geophys. Geochem. Explor.* **12**, 224–227.

PHILOSOPHICAL TRANSACTIONS OF THE ROYAL SOCIETY A MATHEMATICAL, PHYSICAL & ENGINEERING SCIENCES